공학석사학위논문

다양한 질환 심각도 하에서 말초동맥 질환 위치 식별을 위한 딥러닝 기반 도메인 적응 방법 연구

Deep Learning-Based Domain Adaptation Method for Identifying Peripheral Arterial Disease Locations under Various Severity Levels

2022 년 2 월

서울대학교 대학원

기계공학부

이 인 찬

다양한 질환 심각도 하에서 말초동맥 질환 위치 식별을 위한 딥러닝 기반 도메인 적응 방법 연구

Deep Learning-Based Domain Adaptation Method for Identifying Peripheral Arterial Disease Locations under Various Severity Levels

지도교수 윤 병 동

이 논문을 공학석사 학위논문으로 제출함

2021 년 10 월

서울대학교 대학원

기계공학부

이 인 찬

이인찬의 공학석사 학위논문을 인준함

2021 년 12 월

위 원 장 : 김 윤 영 (인)

부위원장 : 윤 병 동 (인)

위 원 : 김 도 년 (인)

Abstract

Deep Learning-Based Domain Adaptation Method for Identifying Peripheral Arterial Disease Locations under Various Severity Levels

In Chan Lee
Department of Mechanical Engineering
The Graduate School
Seoul National University

This paper's primary purpose is to develop a blood pressure waveform (BPW) based deep learning diagnosis model for identifying peripheral arterial disease (PAD) on frequent PAD occurrence arteries. Two issues make it hard to obtain a generalized PAD diagnosis model with a data-driven approach: 1) domain discrepancy resulted from the differences of disease severity and occurring location, 2) data imbalance resulted from the symptomless characteristic of mild PAD. To train a generalized PAD diagnosis model considering practical issues, we propose auxiliary tasks-assisted maximum classifier discrepancy for supervised domain adaptation. The proposed model is validated using virtual patients' BPWs generated from the transmission line model under various disease severity levels. The results show that the proposed model has a superior performance for identifying PAD locations under various disease severity levels. This finding indicates the feasibility of the proposed diagnosis model to real hospitals for identifying the PAD locations in the lower extremities under various disease severity.

Keywords: Cardiovascular Disease
Peripheral Arterial Disease
Pulse Waveform Analysis
Deep Learning
Domain Adaptation

Student Number: 2020-25983

Table of Contents

List of Tables

List of Figures

Nomenclatures

PAD	Peripheral Arterial Disease
ABI	Ankle Brachial Index
ML	Machine Learning
DL	Deep Learning
BPW	Blood Pressure Waveform
MCD	Maximum Classifier Discrepancy
CNN	Convolutional Neural Network
t − SNE	t-Stochastic Neighbor Embedding
Grad CAM	Gradient-weighted Class Activation Mapping
DA	Domain Adaptation
SA	Semantic Alignment
S	Seperation

Chapter 1. Introduction

1.1 Motivation

A disease related to the heart or blood vessels is called cardiovascular disease. Among cardiovascular diseases, those in the arms or legs are called peripheral arterial disease (PAD). PAD is a disease in which plaque accumulates in blood vessels, reducing the amount of blood flow through the blood vessels.

PAD affects 13% of the western population, mostly over 60 years of age [1]-[3]. Because PAD mainly affects elder people, it is expected that PAD will prevail more in the near future due to societal aging. One crucial characteristic of PAD is that it is initially asymptomatic. If symptoms develop, the cure is complex, and mortality increases rapidly [4]. Therefore, it is desirable to address PAD at an early stage through early diagnosis and treatment.

Currently, the most-used method for PAD diagnosis is the Ankle-Brachial Index (ABI) [5], [6]. ABI is the ratio of the maximum blood pressure of the brachial artery (in the arm) and blood pressure in the patient's ankle. PAD can be diagnosed by comparing this index with a reference value. However, ABI is often criticized for its limited accuracy and robustness [7], [8].

Thanks to the development of artificial neural networks, we can train various models with a data-driven approach [9]-[13]. To overcome the weaknesses of ABI, many researchers have used machine learning (ML) and deep learning (DL) approaches based on pulse waveform analysis (PWA) [14]-[17]. PAD alters the propagation and reflection characteristics of the artery affecting the shape of arterial

pulse wave signal (e.g., blood pressure waveform (BPW) and blood flow waveform). Thus, we can obtain information about PAD by analyzing the pulse waveforms. Because pulse waveforms have more information than ABI, a discrete value made by pulse waveform, we can make a more robust and accurate diagnosis result than the conventional ABI method.

Prior research has studied PAD diagnosis by combining deep learning and pulse waveform analysis [18]. However, in this study, the diagnosis was carried out only for abdominal PAD; thus, there is a limitation in that this method cannot diagnose frequently occurring PAD lesions in areas other than the abdomen. For applying PAD screening in public health, it is more important to apprise whether PAD occurs or not.

There are two problems to learn diagnosis model with data-driven approach in real hospitals: 1) a distribution difference of data by the disease location and severity levels [19], [20] and 2) data imbalance between severe and mild PAD patients due to symptomless characteristic. A BPW measured at the peripheral part of the artery is changed by the PAD occurring locations and the disease severity levels. Moreover, it is hard to obtain mild PAD patients' BPW data resulting from the symptomless characteristic in the early stage of PAD. In contrast, the severe PAD patients' data is relatively easy to obtain. For these reasons, it is hard to train a diagnosis model with generalization performance using a naïve data-driven model.

This paper proposes a generalized PAD diagnosis learning method to train a model to screen PAD on frequently PAD occurring lesions considering real hospital situations. We apply a domain adaptation approach to extract domain invariant

features to disease location and severity levels. Then, we validate the generalized diagnosis performance with virtual PAD patients' BPW generated by the transmission line model considering inter and intra individualities.

1.2 Structure of the Thesis

This paper is organized as follows. Section 2 insists on the limitation of the naïve data-driven approach for PAD diagnosing. Then, it describes the main idea of our proposed method. In addition, there is an explanation of our data generation method for describing practical problem situations. Section 3 shows the validation results of our proposed method. Then, section 4 discusses the efficacy of our proposed method. Finally, section 4 concludes this research with suggestions for future works.

Chapter 2. Materials and Methods

2.1 Problem Definition of naïve data-driven approach

The PAD location and severity levels can alter the measure BPW at the peripheral part of an artery. Thus, though PAD occurs at the same artery location, the BPW data can differ according to PAD severity. In other words, there is a domain discrepancy by PAD severity level.

If there is a domain discrepancy between two datasets, the model trained with a data-driven approach shows poor classification performance on the target domain data, which does not appear in the training step. This is because the model trains the classifier to optimize source domain data. To minimize the performance degradation resulting from domain discrepancy, many researchers have studied domain adaptation, extracting domain invariant features to obtain a generalized model.

Inevitably, there is a domain discrepancy in actual hospital data because each patient has their own vascular parameters and severity levels. Moreover, it is hard to derive mild patients' BPW data because of the symptomless characteristic of PAD. In contrast, it is easy to obtain severe patients' BPW data. That is, there are domain discrepancy and data imbalance problems at the same time in real hospitals. Thus, it is hard to make a generalized PAD diagnosis model with a data-driven approach because of domain discrepancy and data imbalance. This paper focuses on developing a robust DL-based PAD location identification method considering real hospital situations using BPWs.

2.2 Proposed Method for Training Generalized PAD Diagnosis Model

2.2.1 Domain Adaptation

If there is a domain discrepancy between two datasets (train and test dataset), the model, which is trained by a data-driven approach, shows poor diagnosis performance on the test dataset [21]-[24]. The model optimizes to classify the train dataset as shown in figure 2-1.

At first, we define domain and class for a clear understanding. The PAD severity level is the domain. Therefore, severe PAD patients' data is source domain data mainly utilized to train the classification task. In contrast, the target domain is Mild PAD patients. Next, the class is PAD occurring locations because our task is to identify PAD lesions. Thus, class is PAD occurring arteries such as Thigh and Calf. In the future description, domain differences are expressed in color, and data classes are expressed in the shape of the data.

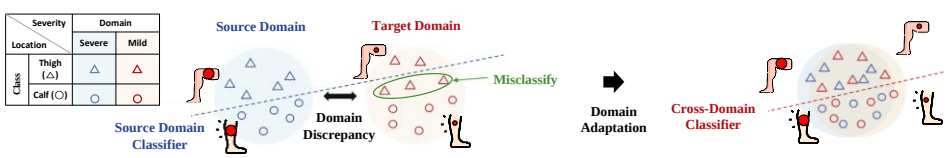

Figure 2-1 Conceptual diagram of domain discrepancy and domain adaptation

If there is a domain discrepancy between two datasets (train and test dataset), the model, which is trained by a data-driven approach, shows poor diagnosis performance on the test dataset [21]-[24]. The model optimizes to classify the train dataset as shown in figure 2-1.

At first, we define domain and class for a clear understanding. The PAD severity level is the domain. Therefore, severe PAD patients' data is source domain data mainly utilized to train the classification task. In contrast, the target domain is Mild PAD patients. Next, the class is PAD occurring locations because our task is to identify PAD lesions. Thus, class is PAD occurring arteries such as Thigh and Calf. In the future description, domain differences are expressed in color, and data classes are expressed in the shape of the data.

2.2.2 Maximum Classifier Discrepancy

Unlike the adversarial-based domain adaptation method, maximum classifier discrepancy (MCD) is known for learning task-specific classifiers [31]. Thus, MCD can learn task-relevant classifiers while extracting domain invariant features.

MCD is a representative unsupervised domain adaptation method considering task-specific decision boundaries. As shown in figure 2-2, the MCD learning method needs a model consists of one feature extractor and two classifiers for manipulating distribution discrepancy.

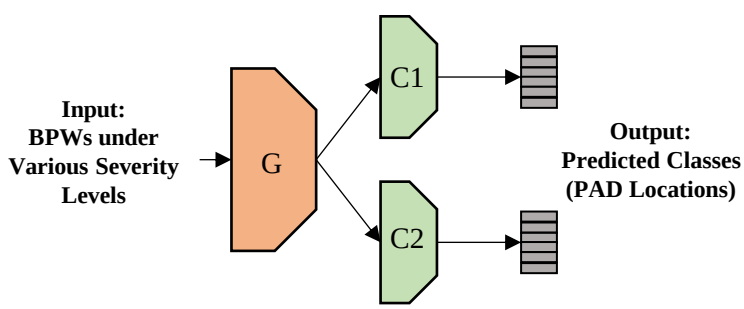

Figure 2-2 The architecture of maximum classifier discrepancy

Figure 2-3 shows the overall training procedure of MCD. As can be seen in the

figure, the MCD learning method is composed of three steps.

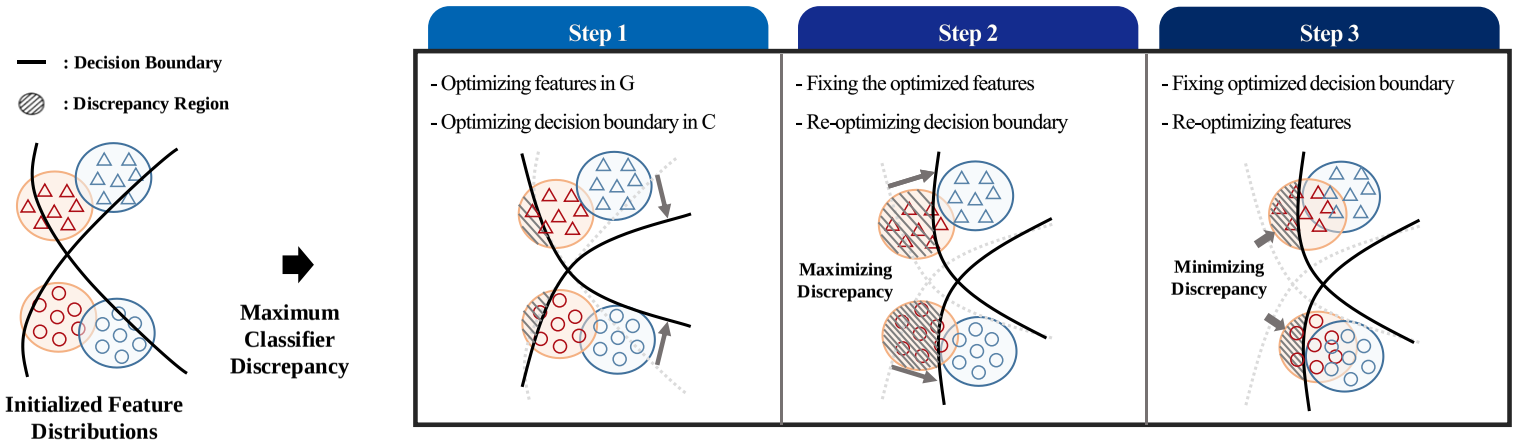

Figure 2-3 Schematic diagram of the training processes of MCD learning method

Step 1: Training on source domain data. As the first step of the MCD, the feature extractor and two classifiers are trained to classify source domain data well. So, after this step, the model can appropriately classify source domain data.

$$L(X_s, T_S) = -E_{x_s, y_s \sim (X_s, Y_s)} \sum_{k=1}^{K} I_{[k=y_s]} log p(y|x_s) \tag{2.1}$$

Step 2: Maximizing domain discrepancy. In this step, only two classifier's weights are updated while the feature extractor's weights are fixed. Two classifiers are trained to predict different classes of target domain data while learning to distinguish the class of the source domain data. In other words, two classifiers are trained to maximize the discrepancy regions in which two classifiers predict different classes about target domain data. Target samples that two classifiers predict differently can have domain-related features extracted by the feature generator.

$$\min_{F1,F2} L(X_s, Y_s) - E_{x_t \sim X_t}\{d(p_1(y|x_t), p_2(y|x_t)\} \tag{2.2}$$

Step 3: Minimizing domain discrepancy. For extracting domain invariant but optimized for classification features, only the feature extractor is updated while two classifiers' weights are fixed. Then, the feature extractor is trained to extract features that can minimize the discrepancy. By doing so, the embedded features of target domain data are much closer to source domain data. Moreover, this learning step repeats N times in the same batch for deriving feature extractor which can extract domain invariant features.

$$\max_{G} E_{x_t \sim X_t}\{d(p_1(y|x_t), p_2(y|x_t)\} \tag{2.3}$$

2.2.3 Proposed Methods

MCD is an unsupervised domain adaptation approach, which cannot be applied to the faced problem. In our faced problem, we have few labeled mild PAD patients' data and a relatively large amount of labeled severe PAD patients' data. Because we have labeled data in both domains, our problem must be solved by a supervised learning method, not unsupervised.

For applying the MCD to our problem while taking advantage of a task-specific classifier, we add two auxiliary tasks: semantic alignment and separation loss [32]. Semantic alignment loss can measure the distance between features with the same label but in different domains. Thus, if we minimize this loss, we can closely embed data features with the same class but different domains. Semantic alignment loss is expressed in equation (2.4)

$$L_{SA}(g) = \sum_{a=1}^{C} d\left(p\left(g(X_a^s)\right), p\left(g(X_a^t)\right)\right) \tag{2.4}$$

On the other hand, separation loss can measure the distance between features with different labels but in the same domain. Therefore, we can faraway embed data features with the same domain but different classes. If we combine these two loss terms, we can expect the synergy effect which increases classification performance as well as decreases domain discrepancy (shown in figure 2-4.).

$$L_S(g) = \sum_{a,b|a\neq b} k\left(p\left(g(X_a^s)\right), p\left(g(X_b^t)\right)\right) \tag{2.5}$$

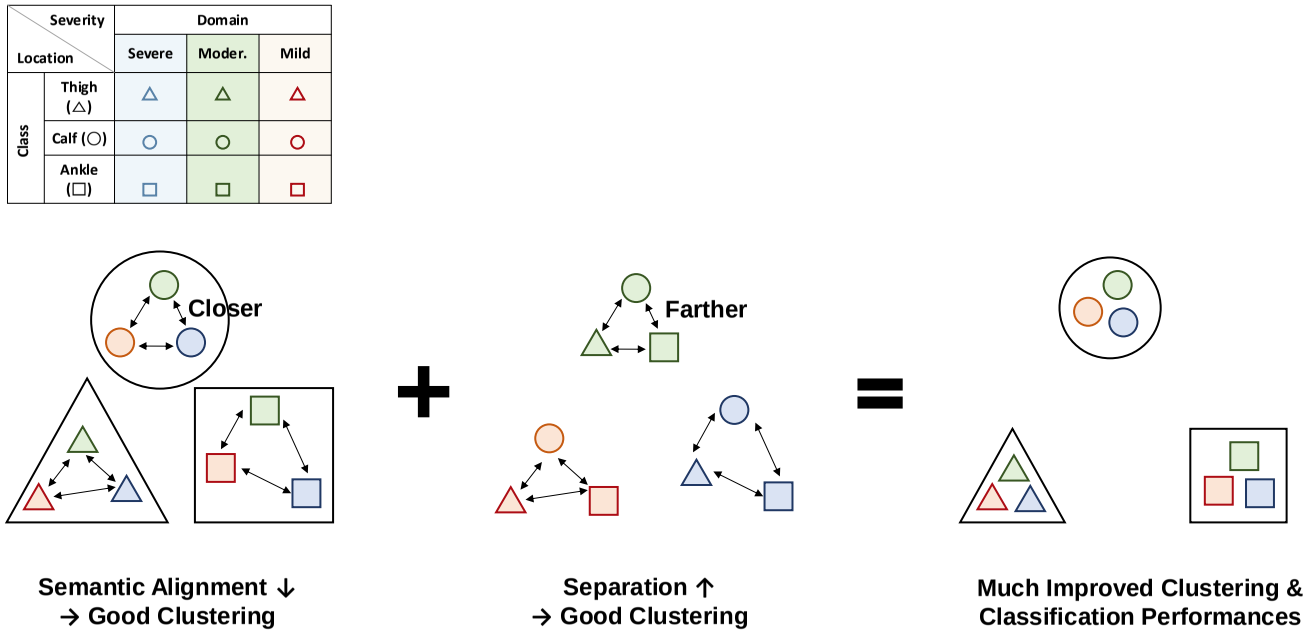

Figure 2-4 Auxiliary tasks: semantic alignment and separation loss

Our proposed loss function is shown in equation (2.6)

$$\min_{G} d(p_1(y|x_t), p_2(y|x_t)) - w * L_{SA}(g) + (1 - w) * L_S(g) \qquad (2.6)$$

The first term of equation (2.6) is original MCD's feature extraction task to minimize the domain discrepancy. Additionally, we add weighted semantic alignment and separation loss to original MCD's loss for increasing classification performance while decreasing domain discrepancy.

For applying the proposed learning method to our task, we utilize CNN architecture composed of a modified Alexnet structure [15]. Figure 2-5 shows the CNN architecture used in our work. This architecture predicts the PAD locations based on the 2ch input composed of blood pressure waveforms measured at arm and ankle. We use an RMSprop optimizer to train our model with a 0.00005 initial learning rate. Also, we set the weight between semantic alignment and separation loss as 0.1 and the number of repetitions as 8 in step 3.

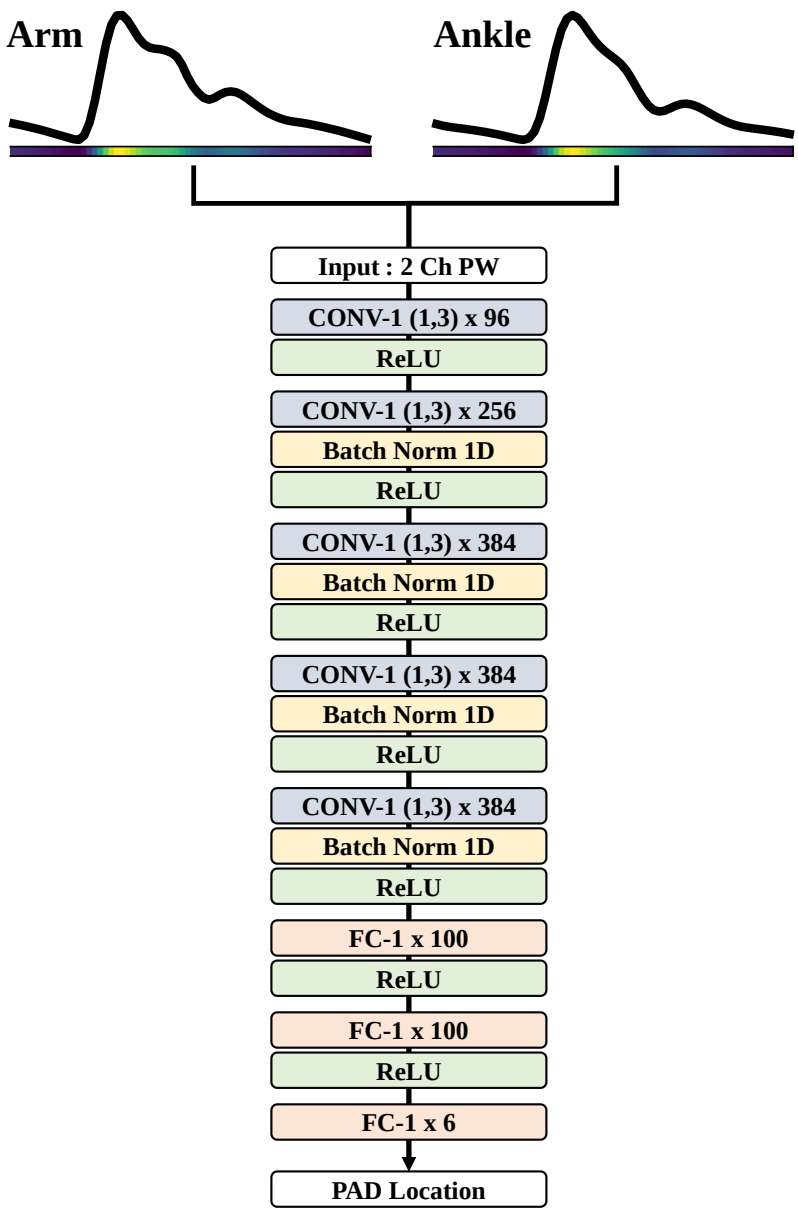

Figure 2-5 A CNN architecture for PAD diagnosis

2.3 Virtual PAD Patients' BPW Data Generation

2.3.1 Transmission Line Model

We use the simulation model used in early work[34],[35] to generate blood pressure waveform data. This model combines the modified Noordergraaf's 55 segments arterial model[36] and transmission line model. The model simulates blood flow and blood pressure with blood vessel parameters based on hemodynamics. Blood pressure and blood flow can be calculated using the following equations.

$$P_{outlet} = P_{inlet}(1 + \Gamma)/\left(e^{\gamma l} + \Gamma e^{-\gamma l}\right)$$

$$F_{outlet} = F_{inlet}(1 - \Gamma)/\left(e^{\gamma l} - \Gamma e^{-\gamma l}\right)$$

where γ is a propagation coefficient that is determined by the geometric and physical properties of the artery. Γ is a reflection coefficient that is determined by the branching and impedance of blood vessels. Also, l represents the length of each blood vessel segment. Blood pressure and blood flow are connected by input impedance, as shown in the following equation.

$$P_{inlet} = F_{inlet} Z_{input} = F_{inlet} Z_C \frac{\left(e^{\gamma l} + \Gamma e^{-\gamma l}\right)}{\left(e^{\gamma l} - \Gamma e^{-\gamma l}\right)}$$

Therefore, the blood pressure or blood flow in all branches can be calculated by using the blood pressure or blood flow data in one blood vessel, using above equations.

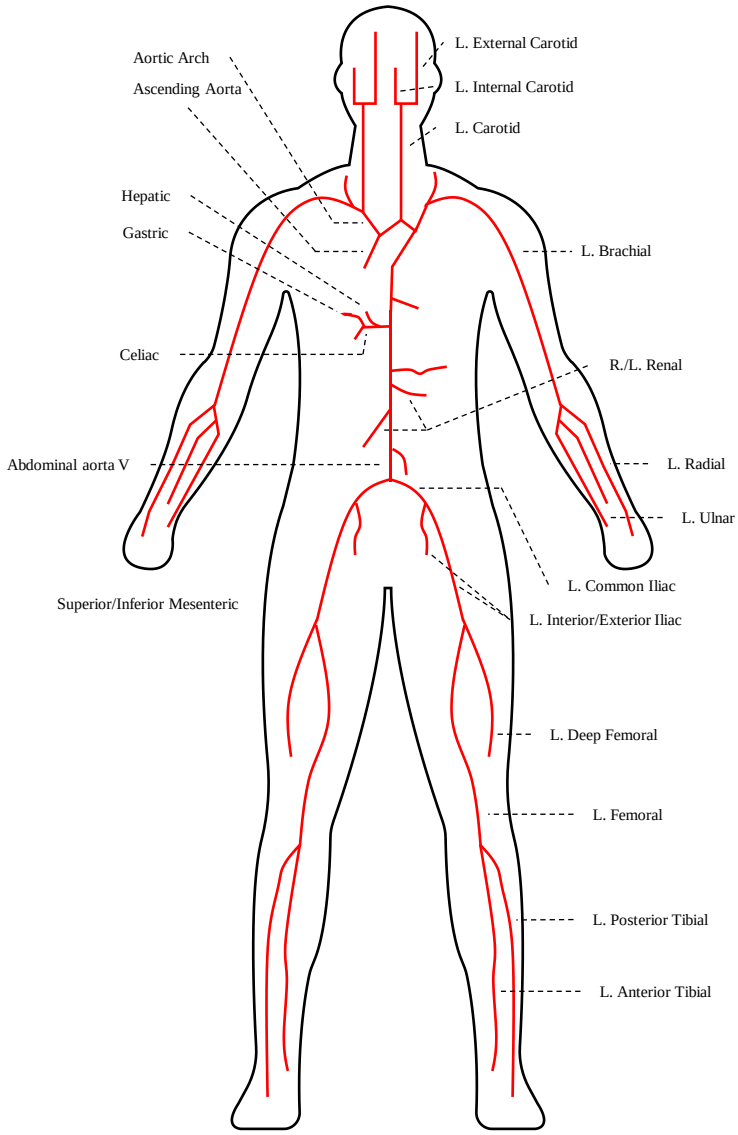

Figure 2-6 Arterial tree

Table 2 - 1 Number and name of 55 segments of arterial tree

Segment number	Arterial segment name	Segment number	Arterial segment name
1	Ascending aorta	29	Abdominal aorta III
2	Aortic arch I	30	Left renal
3	Brachiocephalic	31	Abdominal aorta IV
4	Right subclavian I	32	Inferior mesenteric
5	Right carotid	33	Abdominal aorta V
6	Right vertebral	34	Right common iliac
7	Right subclavian II	35	Right external iliac
8	Right radius	36	Right internal iliac
9	Right ulna I	37	Right deep femoral
10	Aortic arch II	38	Right femoral
11	Left carotid	39	Right external carotid
12	Thoracic aorta I	40	Left internal carotid
13	Thoracic aorta II	41	Right posterior tibial
14	Intercostals	42	Right anterior tibial
15	Left subclavian I	43	Right interosseous
16	Left vertebral	44	Right ulnar II
17	Left subclavian II	45	Left ulnar II
18	Left ulnar I	46	Left interosseous
19	Left radius	47	Right internal carotid
20	Celiac I	48	Left external carotid
21	Celiac II	49	Left common iliac
22	Hepatic	50	Left external iliac
23	Splenic	51	Left internal iliac
24	Gastric	52	Left deep femoral
25	Abdominal aorta I	53	Left femoral
26	Superior mesenteric	54	Left posterior tibial
27	Abdominal aorta II	55	Left anterior tibial
28	Right renal		

2.3.2 Setting for Virtual PAD Patients

For simulating virtual PAD patients' BPWs using multibranch transmission line model, we consider various virtual patients which has different vascular parameters.

The geometric and physical vascular parameters that have a great influence on blood pressure or blood flow are arterial radius (R), length (L), Young's modulus (E), wall thickness(T), and peripheral resistance (PR). Combination of these five major vascular parameters can be used to describe a variety of people. In addition, it is possible to generate blood pressure waveforms of various people by putting a combination of the five blood vessel parameters as inputs to the simulation model.

According to the previous study [8], the values of the major vascular parameters were set as 5 representative values of the normal category, respectively. Therefore, a total of 3,125 individuals were generated through a combination of each parameter (5^5).

To reflect uncertainties in measurement of BPWs, we set the main vascular parameters coefficient of variation as 0.01. Therefore, one patient's simulated BPWs can be vary from simulation to simulation. We simulate 10 BPWs with uncertainty for each patient. Figure 2.7 shows the schematic diagram of virtual PAD patients generation considering inter and intra individualities.

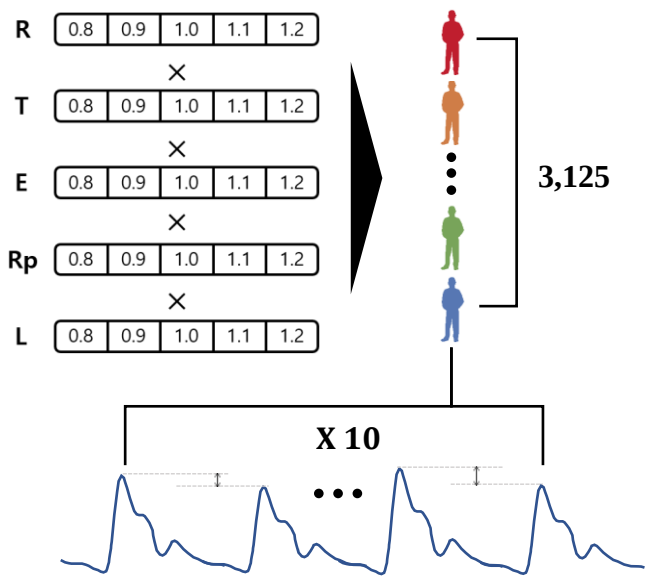

Figure 2-7 The schematic diagram of virtual PAD patients generation

We generated blood pressure waveforms of normal individuals and PAD patients who had PAD in 5 representative frequent PAD sites. PAD is described as the situation in which the radius of the PAD-affected artery is reduced. The severity of the disease was defined as a decreased radius, as compared to the original radius. For example, if the size of the original radius is reduced by 60%, the severity is defined as 60%.

2.3.3 Data Description

We generate virtual PAD patients by implementing 6 disease statuses (1 normal and 5 representative PAD status) to virtual individuals made by combinations of 5 main vascular parameters. These virtual PAD patients' arm and ankles BPWs generated through multibranch transmission line model.

Among 3,125 virtual individuals, 3,000 individuals are severe PAD patients, 62 individuals are mile PAD patients, and 63 individuals set mild PAD patients for validating diagnosis model performance. We assumed that each individual has only one randomly selected PAD disease status. Then, 10 BPWs of each patient were measured. Here, Severe PAD patients' severity range is 50-60% and mild PAD patients' severity range is 20-30%. The Severity level is distributed randomly in a set severity range.

Test Dataset consists of specific severity levels (20, 30, 40, 50%). For validating generalized performance of diagnosis model, each severity test data is composed of all possible case of virtual PAD patients. In other words, each individual virtual PAD patients can have 6 PAD disease statuses.

Table 2-2 shows the summary of the generated datasets which is used for training(source, target, and validation data).

Table 2 - 2 Training and test dataset

Training Dataset	**Severe PAD Patients (Source)**						**Mild PAD Patients (Target)**						**Mild PAD Patients (Validation)**					
Patient Number	**3,000**						**62**						**63**					
Severity Level	**50 ~ 60 %**						**20 ~ 30 %**						**20 ~ 30 %**					
PAD Location (Patient Number)	**N**	**33**	**49**	**50**	**53**	**55**	**N**	**33**	**49**	**50**	**53**	**55**	**N**	**33**	**49**	**50**	**53**	**55**
	496	**522**	**469**	**523**	**478**	**513**	**9**	**10**	**12**	**15**	**6**	**9**	**17**	**10**	**7**	**9**	**12**	**7**

2.4 Overall Procedure

Figure 2-8 shows the overall flowchart of the our work. The flowchart is largely composed of 3 step: data generation, diagnosis model training, and diagnosis model testing.

The first step of data generation is virtual PAD patient generation considering inter-individuality and PAD locations. The generated virtual PAD patients are assigned to the source and target domains. Then, generated virtual PAD patients are used as an input to the transmission line model considering intra -individuality for simulating the BPWs. Train, validation, and test dataset are generated by doing this procedure.

In the training step, after initializing the model, learning is performed according to the training step described in 2.2.2. At first, the model is trained to maximize classification performance on source domain data. Then, the two classifiers are trained to maximize target domain discrepancy while the feature extractor's weights are fixed. The feature extractor is trained to minimize target domain discrepancy while two classifiers are frozen in the last step. Here, step 3 is N times repeated for one minibatch.

In the last diagnosis model testing step, we test the model which shows the lowest loss in the training. Here we use a test dataset having all six PAD states for validating the PAD diagnosis accuracy.

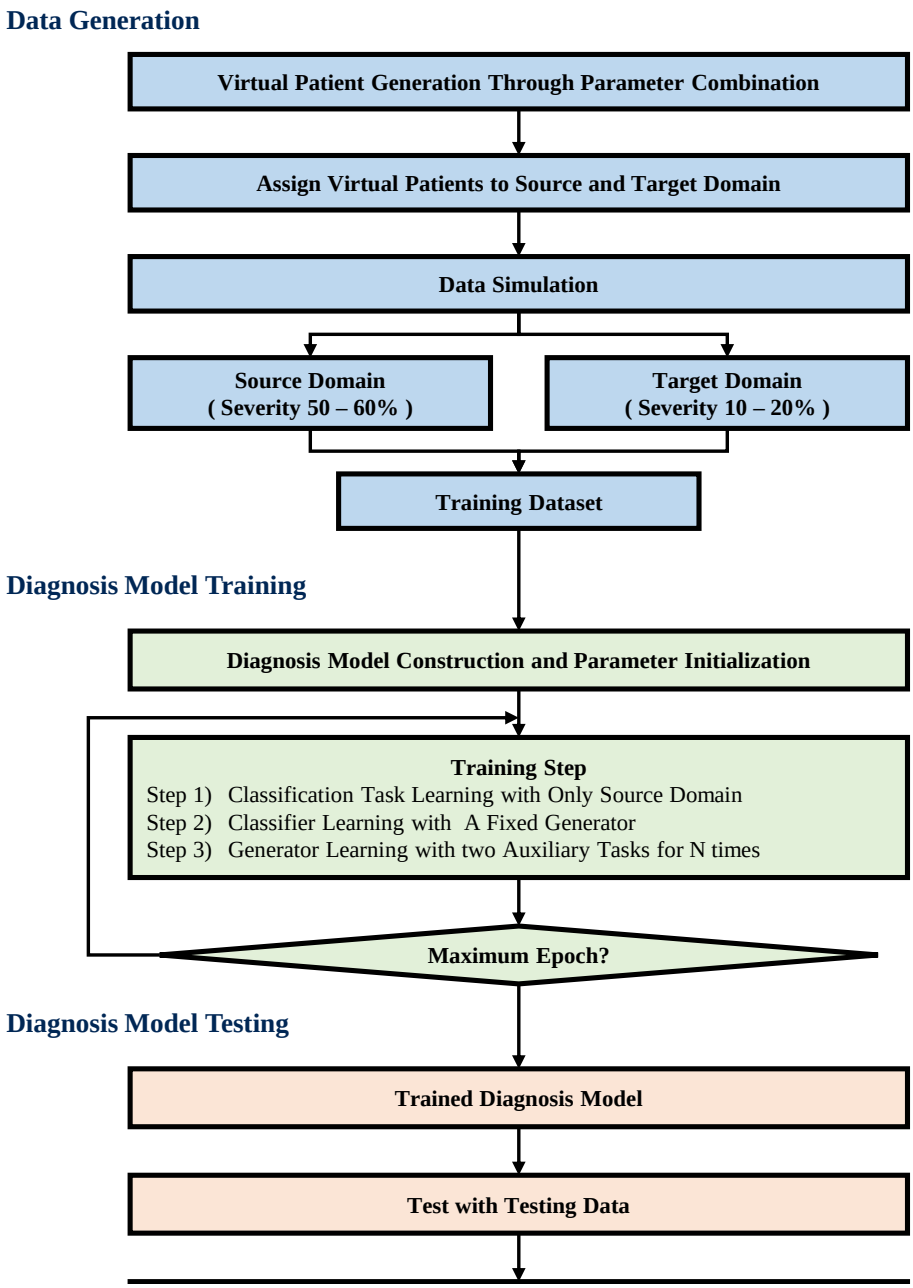

Figure 2-8 Flowchart of the proposed method

Chapter 3. Results

3.1 Compared Methods

To verify the effectiveness of our proposed method, the diagnosis performance of other CNN-based learning methods were compared: (1) vanilla supervised learning method with only source domain data (2) vanilla supervised learning method with source and target domain data. (3) supervised domain adaptation learning method with source and target domain data [14]. (4) proposed learning method with source wand target domain data. Above 4 learning methods are trained with CNN architecture shown in figure 2.5. We trained 100 models for each learning method.

3.2 Results

Table 3-1 shows the average diagnosis accuracy of four learning methods. Also, figure 3-1 shows the bar plots with average diagnosis performance of four learning methods. Figure 3-2 compares the latent space of four methods via t-distributed Stochastic Neighbor Embedding (t-SNE)[37]. Via gradient-weighted class activation mapping (Grad CAM), figures 3-3 and 3-4 present feature importance by disease severity levels of diagnosis model with domain adaptation and without domain adaptation [38]. Figure 3-5 compares the confusion matrix of (a) without domain adaptation model with 30% severity test dataset, (b) without domain adaptation model with 50% severity test dataset, (c) with domain adaptation model with 30% severity test dataset, (d) with domain adaptation model with 50% severity test dataset

Table 3 - 1 Diagnosis results comparison of four learning methods

Learning Methods	Accuracy (%)			
	30% SL	35% SL	40% SL	45% SL
Source Only (No DA)	25.11± 5.55	35.79±6.83	56.23±5.69	83.31±5.90
Source + Target (No DA)	65.33±4.38	72.19±3.54	78.42±2.64	91.73±3.71
Source + Target with SA & S	73.92±5.02	82.16±5.42	89.71±5.95	93.98±7.02
Proposed method	**89.41±2.65**	**93.88±2.28**	**96.33±2.73**	**97.18±3.45**

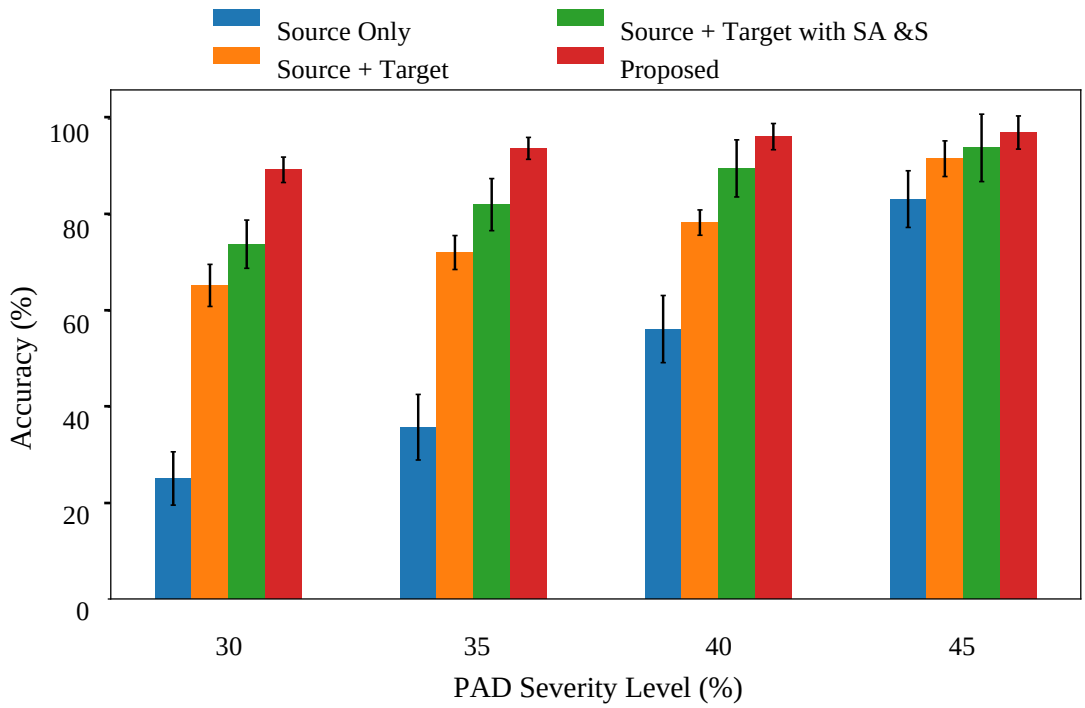

Figure 3-1 Average diagnosis accuracy of each method

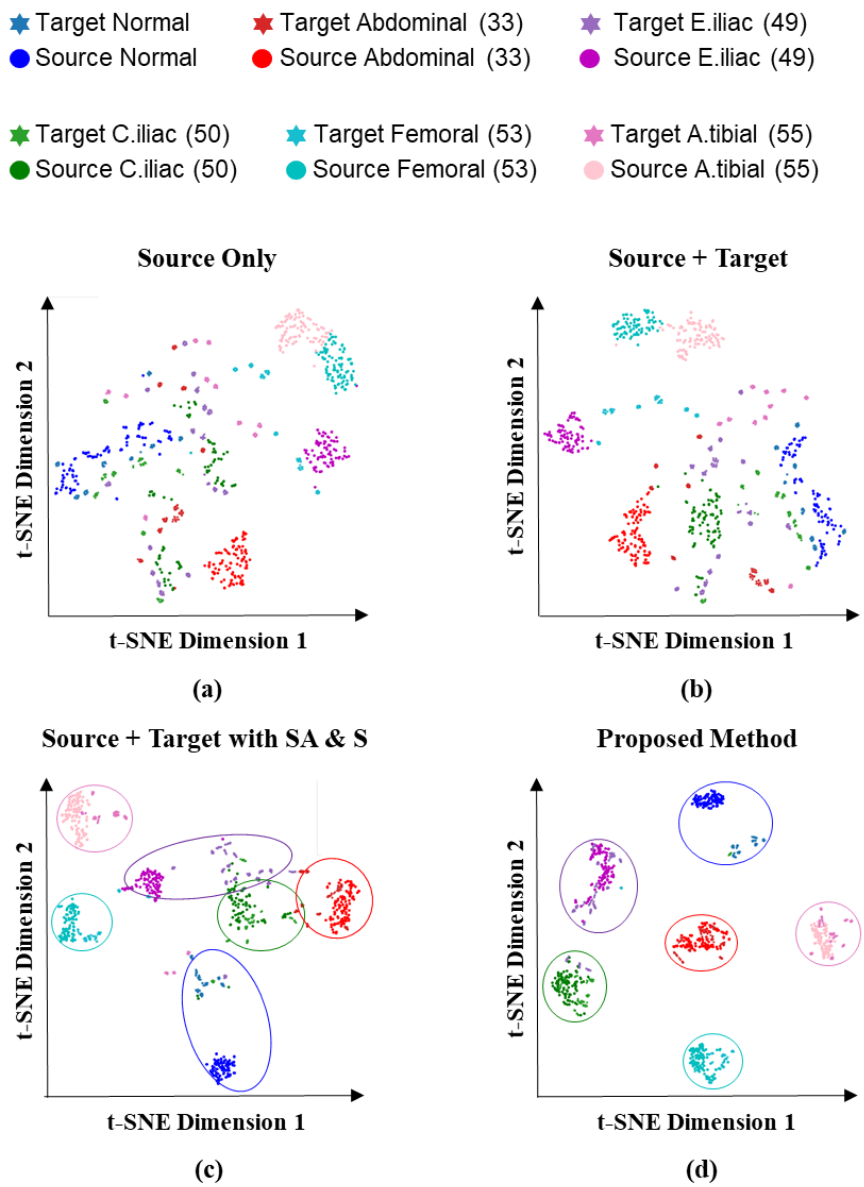

Figure 3-2 Latent space visualization via t-SNE of (a) vanilla supervised learning method with only source domain data (b) vanilla supervised learning method (c) supervised domain adaptation learning method. (d) proposed learning method

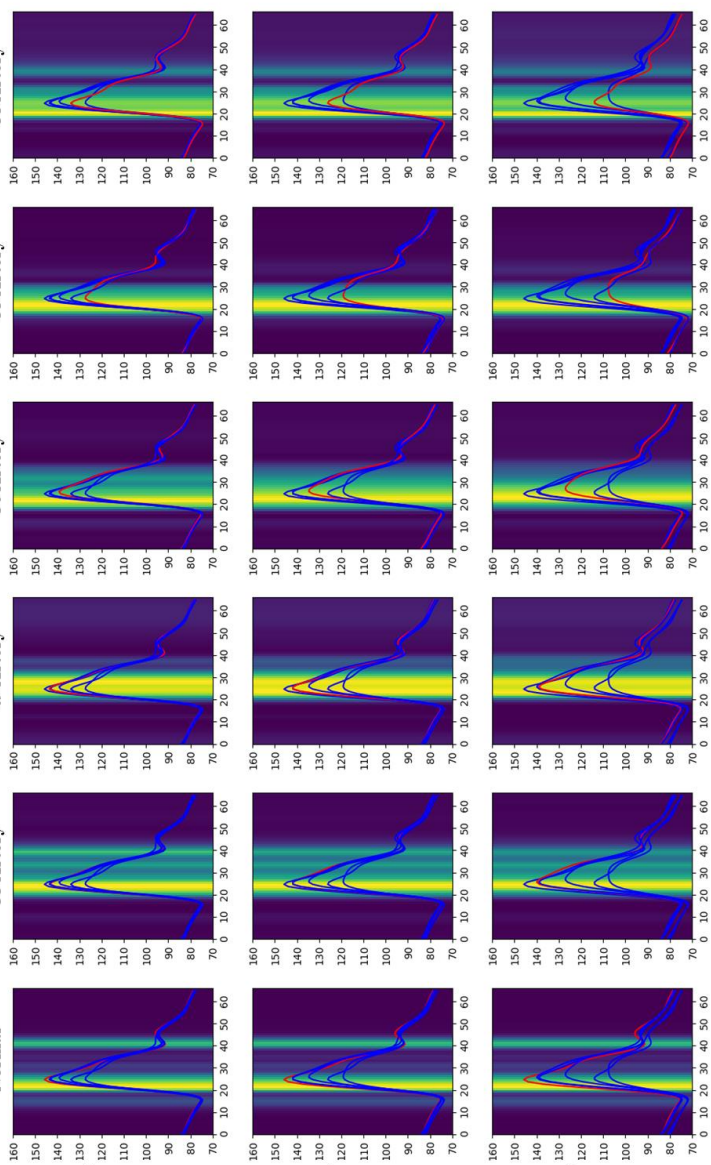

Figure 3-3 Feature importance of proposed learning method represented by GradCAM

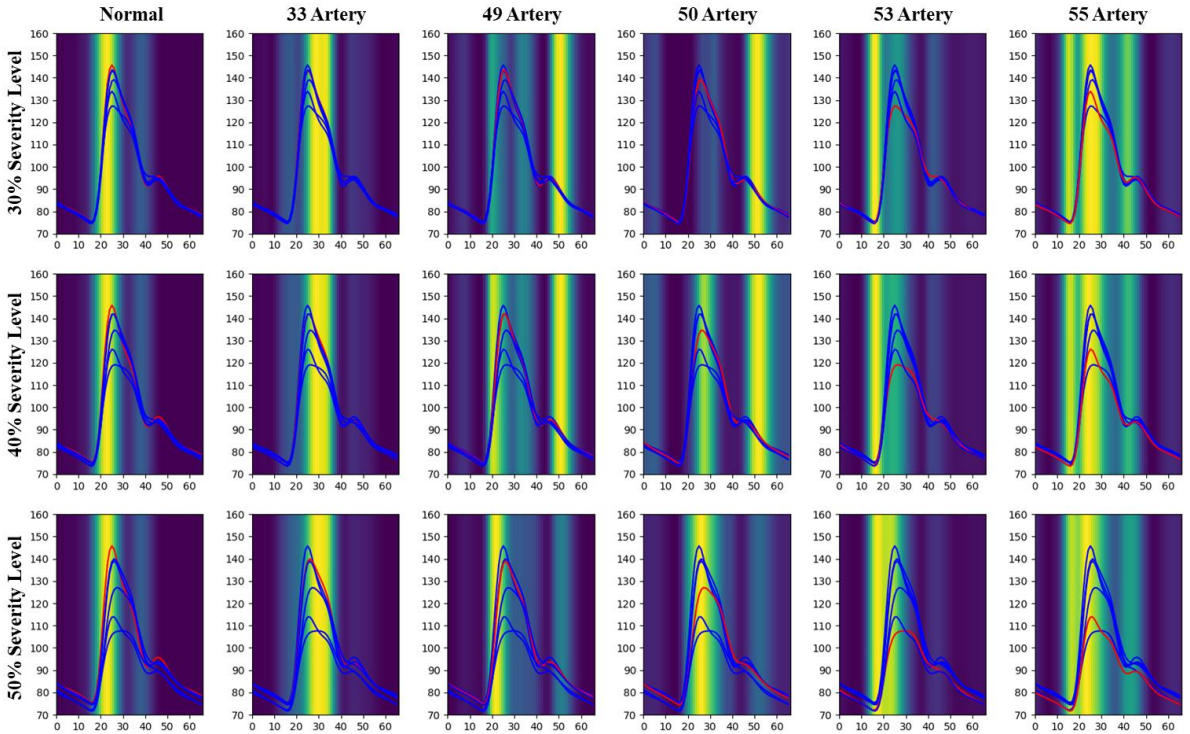

Figure 3-4 Feature importance of supervised learning method without domain adaptation represented by GradCAM

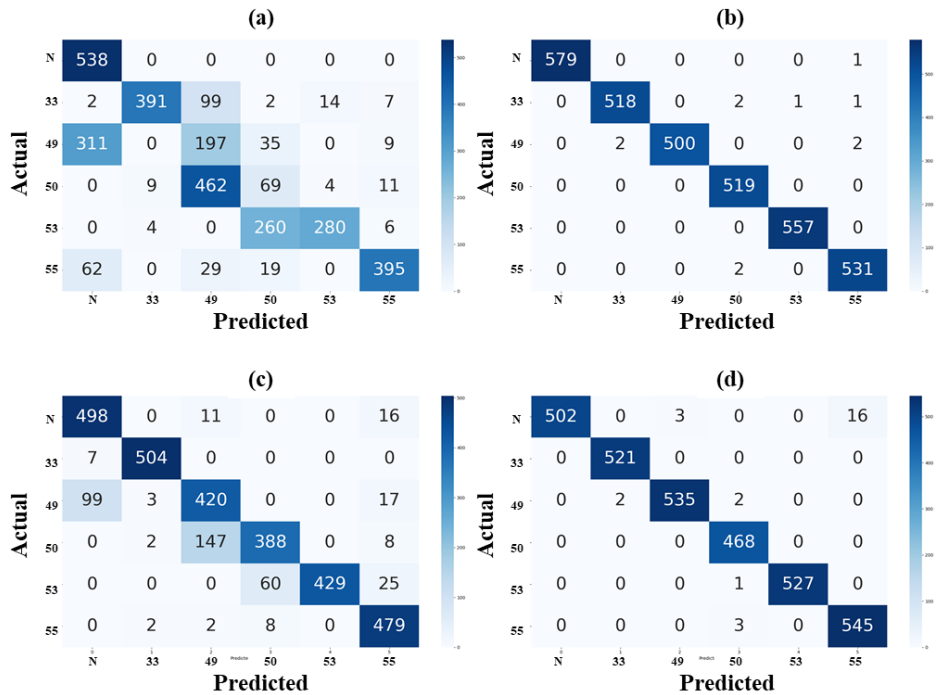

Figure 3-5 Confusion matrix of (a) vanilla supervised learning method with 30% severity level, (b) vanilla supervised learning method with 50% severity level, (c) proposed learning method tested with 30% severity level, (d) proposed learning method tested with 50% severity level.

Chapter 4. Discussion

4.1 Efficacy of Proposed Learning Method

From table 3-1 and figure 3-1, our proposed model shows the highest classification performance in all severity of test datasets. We can find that the lower the test data's severity level, the lower the diagnosis accuracy of models. This is because the lower the severity level, the larger the difference of data distribution with source domain data. Therefore, the domain adaptation applied models ((3), (4)) outperform the two vanilla models ((1), (2)), which do not contain domain adaptation.

We can understand the performance difference of models through feature space visualization via t-Stochastic Neighbor Embedding. Figure 3-2 (a), (b) shows the feature space of vanilla CNN models ((1), (2)) in which domain adaptation is not applied. It is hard to make a cluster and classify the class of the target domain data. The diagnosis performance is relatively bad because these two models' features are embedded poorly in the feature space. On the other hand, model (3)'s feature space is much more straightforward than (1) and (2). As shown in figure 3-2 (c), source and target domain data with the same class are clustered well in the latent space. Also, it is easy to differentiate the cluster's class by looking at the feature space. Model (4)'s feature space is shown in figure 3-2 (d). In this figure, the cluster looks clear, and the distance between each cluster is appropriate. Therefore, we can easily identify the data's class by looking at the latent space. Thus, we can infer that the diagnosis performances of models (3),(4) are superior to that of models (1) and (2) by the figure 3-2.

4.2 Effects of Domain Adaptation

To understand how domain adaptation affects the diagnosis performance of the model, Grad CAM is applied to model (2) and model (4), to which domain adaptation is not applied and applied, respectively. Figure 3-3 and 3-4 are the results showing which places are considered essential when predicting the class of each severity level test dataset by applying Grad CAM to models 4 and 2, respectively. In the case of model 4, to which Domain adaptation is applied, classification is performed focusing on the same place for each class even if the severity of the test data varies. On the other hand, in the case of model 2, to which domain adaptation is not applied, the model focus on 49 and 50 artery PAD differs depending on the severity. We can estimate that inconsistency also affects the classification results from the confusion matrix shown in figure 3-5

In Figure 3-5, it can be confirmed that the conformation matrix (b), (d) of the two models for the 50% Severity test dataset is very clean. On the other hand, confusion matrix (a), (c) of the two models for the 30% severity test dataset are somewhat massive. First, it may be seen from (a) that many misclassifications are made for 49 and 50 artery PADs. In other words, there are many misclassifications of the actual 49 and 50 artery PAD data, and the actual 53 artery PAD is misclassified as well. On the other hand, in the case of (c), to which domain adaptation is applied, this misclassification has been significantly reduced. The model misclassified normal and 49 arteries PAD, 49 and 50 artery PAD. For this part, misclassification may be performed due to measurement uncertainty in data sets with low severity.

Figures 3-3 and 3-4 show that when domain adaptation is applied, characteristics

that remain unchanged according to the severity of the disease are extracted. In addition, through the analysis of Figure 3-5, it was confirmed that these characteristics had a positive effect on disease classification.

4.3 Potential for Practical Applicability

As discussed in 4.1, the diagnostic performance of the proposed method is superior to that of other models. In addition, patients with a 30% severity level can be diagnosed with high accuracy about 90%. Compared to the other models, the diagnostic accuracy does not differ much as the severity level decreases. As discussed in 4.2, this is because features irrelevant to the severity of the disease are selected and used for classification in the model (4).

According to previous studies, when the severity of PAD reaches around 60%, patients feel symptoms. ABI can be effectively applied to detect PAD from this point on. However, it is known that there are problems in terms of accuracy and reliability in diagnosing PAD at a severity level of less than 50% with ABI. On the other hand, our proposed deep learning-based PAD diagnostic model can diagnose both severe patients and 30% severity level patients with high accuracy above 90%. In other words, it is possible to diagnose early patients with PAD that cannot be detected with the conventional diagnostic model ABI. Therefore, if the proposed method is used for an actual diagnosis, it is expected to contribute to the promotion of national health through the early diagnosis of PAD.

Chapter 5. Conclusions

5.1 Summary and Contributions

This paper proposes a deep learning-based domain adaptation method for identifying PAD locations under various severity levels. To minimize domain discrepancy resulted from disease severity difference while utilizing few labeled target domain data, we propose auxiliary tasks-assisted maximum classifier discrepancy for supervised domain adaptation. The proposed method was demonstrated using virtual patients' BPWs data considering domain discrepancy and data imbalance. The results show that the proposed method offers the best accuracy for PAD location identification. The t-SNE results showed that our proposed method exhibits distinctive feature space. Moreover, using Grad CAM, we investigated the input importance and found that our proposed model can extract domain invariant features.

Contribution 1: First research for identifying PAD occurring locations

This is the first study for identifying PAD occurring locations. Previous studies have focus on the disease detection at one artery location. Many researchers studied about disease severity level estimation. However, it is more critical for applying practical health screening to detect PAD on PAD frequently occurring arteries than PAD disease severity regression. Therefore, we developed a deep learning-based PAD location diagnostic model based on the fact that when PAD occurs, blood pressure waveforms are deformed. If these diagnostic methods are actually applied, they can be used for primary care, such as the health screening system, to promote national health. In addition, it is expected that it will be able to preoccupy the digital

healthcare market by installing the proposed method to wearable devices.

Contribution 2: Auxiliary tasks-assisted MCD for supervised domain adaptation

Unlike adversarial domain adaptation, MCD is an unsupervised learning method that learns task-specific decision boundaries. However, since label information of the target domain is given in the faced problem, a supervised learning method is needed to use the information efficiently. Therefore, two additional tasks were added to utilize most of the label information of the target domain while maintaining the advantage of learning task-specific decision boundaries. As a result, the domain disparity decreased, and the classification performance increased, efficiently solving the problems faced.

Contribution 3: Development of robust PAD diagnosis model considering practical issues (domain discrepancy, data imbalance)

There are many things to consider for applying the PAD diagnosis model: 1) Inter- individuality, 2) intra individuality, 3) domain discrepancy 4) data imbalance. We consider all of these things in the data generation step. Therefore, our proposed method suggests the feasibility of a generalized PAD diagnosis model considering practical issues.

5.2 Suggestions for Future Research

Based on the research conducted in this work, we can present future research in three directions.

Issue 1: Applying the suggested method to other cardiovascular diseases.

We developed a new supervised learning method by adding two auxiliary tasks to the existing MCD method. Our proposed method can be applied to diagnose various cardiovascular diseases that can be diagnosed using pulse waveform analysis. For example, it can be applied to Abdominal aortic aneurysms, where the blood pressure waveform measured at the distal end changes when it occurs. It is expected to solve the problem of domain discrepancy and data imbalance by applying the proposed method to these cardiovascular diseases.

Issue 2: Verification of the proposed method based on real patient data in hospital.

Although several realistic situations such as inter and intra individualities, domain discrepancy, and data imbalance have been considered, there will be more significant uncertainty in actual patient data. Therefore, before applying the proposed method to primary care, it is necessary to verify the trained diagnosis model with actual patient data. When this verification is completed, various studies can be conducted to apply the technology to actual medical diagnoses.

Issue 3: Domain adaptation: Simulation data as a source and real patient data as a target.

Obviously, there will be a difference in data distribution between actual patient data and simulation data acquired in the transmission line model. We can acquire a blood pressure waveform of a virtual patient that is close to infinity. Therefore, setting the verified simulation data to the source domain and the actual patient data

to the target domain will allow us to learn a PAD diagnostic model with generalized performance.

References

1. Morley R L, Sharma A, Horsch A D, Hinchliffe R J. Peripheral artery disease BMJ 2018; 360

2. Criqui, M. H. (2001). Peripheral arterial disease-epidemiological aspects. Vascular medicine, 6(1_suppl), 3-7.

3. Sigvant, B., Wiberg-Hedman, K., Bergqvist, D., Rolandsson, O., Andersson, B., Persson, E., & Wahlberg, E. (2007). A population-based study of peripheral arterial disease prevalence with special focus on critical limb ischemia and sex differences. Journal of vascular surgery, 45(6), 1185-1191.

4. McGrae McDermott M, Greenland P, Liu K, et al. Leg Symptoms in Peripheral Arterial Disease: Associated Clinical Characteristics and Functional Impairment. JAMA. 2001;286(13):1599–1606.

5. Grenon, S. M., Gagnon, J., & Hsiang, Y. (2009). Ankle–brachial index for assessment of peripheral arterial disease. N Engl J Med, 361(19), e40.

6. Stephens, J., Hagler, D., & Clark, E. (2011). Got PAD? Hidden dangers revealed with ABI. Journal of Vascular Nursing, 29(4), 153-157.

7. Khan, T. H., Farooqui, F. A., & Niazi, K. (2008). Critical review of the ankle brachial index. Current cardiology reviews, 4(2), 101-106.

8. Nelson, M. R., Quinn, S., Winzenberg, T. M., Howes, F., Shiel, L., & Reid, C. M. (2012). Ankle-Brachial Index determination and peripheral arterial disease

diagnosis by an oscillometric blood pressure device in primary care: validation and diagnostic accuracy study. BMJ open, 2(5), e001689.

9. Pal, S. K., & Mitra, S. (1992). Multilayer perceptron, fuzzy sets, classifiaction.

10. He, K., Zhang, X., Ren, S., & Sun, J. (2016). Deep residual learning for image recognition. In Proceedings of the IEEE conference on computer vision and pattern recognition (pp. 770-778).

11. Goodfellow, I., Pouget-Abadie, J., Mirza, M., Xu, B., Warde-Farley, D., Ozair, S., ... & Bengio, Y. (2014). Generative adversarial nets. Advances in neural information processing systems, 27.

12. Zhao, Z. Q., Zheng, P., Xu, S. T., & Wu, X. (2019). Object detection with deep learning: A review. IEEE transactions on neural networks and learning systems, 30(11), 3212-3232.

13. Van Houdt, G., Mosquera, C., & Nápoles, G. (2020). A review on the long short-term memory model. Artificial Intelligence Review, 53(8), 5929-5955.

14. Ghasemi, Z., Lee, J. C., Kim, C. S., Cheng, H. M., Sung, S. H., Chen, C. H., ... & Hahn, J. O. (2018). Estimation of cardiovascular risk predictors from non-invasively measured diametric pulse volume waveforms via multiple measurement information fusion. Scientific reports, 8(1), 1-11.

15. Kim, S., Hahn, J. O., & Youn, B. D. (2021). Deep Learning-Based Diagnosis of Peripheral Artery Disease via Continuous Property-Adversarial Regularization: Preliminary in Silico Study. IEEE Access, 9, 127433-127443.

16. Xiao, H., Avolio, A., & Huang, D. (2016). A novel method of artery stenosis diagnosis using transfer function and support vector machine based on transmission line model: A numerical simulation and validation study. Computer methods and programs in biomedicine, 129, 71-81.

17. Kim, S., Hahn, J. O., & Youn, B. D. (2020). Detection and severity assessment of peripheral occlusive artery disease via deep learning analysis of arterial pulse waveforms: Proof-of-concept and potential challenges. Frontiers in bioengineering and biotechnology, 8, 720.

18. Kim, S., Hahn, J. O., & Youn, B. D. (2021). Deep Learning-Based Diagnosis of Peripheral Artery Disease via Continuous Property-Adversarial Regularization: Preliminary in Silico Study. IEEE Access, 9, 127433-127443.

19. Lewis, J. E., Williams, P., & Davies, J. H. (2016). Non-invasive assessment of peripheral arterial disease: Automated ankle brachial index measurement and pulse volume analysis compared to duplex scan. SAGE Open Medicine, 4, 2050312116659088.

20. Rutherford, R. B., Lowenstein, D. H., & Klein, M. F. (1979). Combining segmental systolic pressures and plethysmography to diagnose arterial occlusive disease of the legs. The American Journal of Surgery, 138(2), 211-218.

21. Kouw, W. M., & Loog, M. (2018). An introduction to domain adaptation and transfer learning. arXiv preprint arXiv:1812.11806.

22. Tao, J., Chung, F. L., & Wang, S. (2012). On minimum distribution discrepancy support vector machine for domain adaptation. Pattern Recognition, 45(11), 3962-3984.

23. Lu, C., Gu, C., Wu, K., Xia, S., Wang, H., & Guan, X. (2020). Deep transfer neural network using hybrid representations of domain discrepancy. Neurocomputing, 409, 60-73.

24. Zhou, Q., Wang, S., & Xing, Y. (2021). Multiple adversarial networks for unsupervised domain adaptation. Knowledge-Based Systems, 212, 106606.

25. Tzeng, E., Hoffman, J., Saenko, K., & Darrell, T. (2017). Adversarial discriminative domain adaptation. In Proceedings of the IEEE conference on computer vision and pattern recognition (pp. 7167-7176).

26. Wang, X., & Liu, F. (2020). Triplet loss guided adversarial domain adaptation for bearing fault diagnosis. Sensors, 20(1), 320.

27. Ben-David, S., Blitzer, J., Crammer, K., & Pereira, F. (2006). Analysis of representations for domain adaptation. Advances in neural information processing systems, 19.

28. Chen, C., Chen, Z., Jiang, B., & Jin, X. (2019). Joint domain alignment and discriminative feature learning for unsupervised deep domain adaptation. In Proceedings of the AAAI conference on artificial intelligence (Vol. 33, No. 01, pp. 3296-3303).

29. Ma, P., Zhang, H., Fan, W., & Wang, C. (2020). A diagnosis framework based

on domain adaptation for bearing fault diagnosis across diverse domains. ISA transactions, 99, 465-478.

30. Ganin, Y., Ustinova, E., Ajakan, H., Germain, P., Larochelle, H., Laviolette, F., ... & Lempitsky, V. (2016). Domain-adversarial training of neural networks. The journal of machine learning research, 17(1), 2096-2030.

31. Saito, K., Watanabe, K., Ushiku, Y., & Harada, T. (2018). Maximum classifier discrepancy for unsupervised domain adaptation. In Proceedings of the IEEE conference on computer vision and pattern recognition (pp. 3723-3732).

32. Motiian, S., Piccirilli, M., Adjeroh, D. A., & Doretto, G. (2017). Unified deep supervised domain adaptation and generalization. In Proceedings of the IEEE international conference on computer vision (pp. 5715-5725).

33. Krizhevsky, A., Sutskever, I., & Hinton, G. E. (2012). Imagenet classification with deep convolutional neural networks. Advances in neural information processing systems, 25.

34. He, W., Xiao, H., & Liu, X. (2012). Numerical simulation of human systemic arterial hemodynamics based on a transmission line model and recursive algorithm. Journal of Mechanics in Medicine and Biology, 12(01), 1250020.

35. Xiao, H., Avolio, A., & Zhao, M. (2016). Modeling and hemodynamic simulation of human arterial stenosis via transmission line model. Journal of Mechanics in Medicine and Biology, 16(05), 1650067.

36. Liang, F., Takagi, S., Himeno, R., & Liu, H. (2009). Multi-scale modeling of the human cardiovascular system with applications to aortic valvular and arterial stenoses. Medical & biological engineering & computing, 47(7), 743-755.

37. Van der Maaten, L., & Hinton, G. (2008). Visualizing data using t-SNE. Journal of machine learning research, 9(11).

38. Selvaraju, R. R., Cogswell, M., Das, A., Vedantam, R., Parikh, D., & Batra, D. (2017). Grad-cam: Visual explanations from deep networks via gradient-based localization. In Proceedings of the IEEE international conference on computer vision (pp. 618-626).

Abstract (Korean)

다양한 질환 심각도 하에서 말초동맥 질환 위치 식별을 위한 딥러닝 기반 도메인 적응 방법 연구

서울대학교 공과대학
기계공학부 대학원
이 인 찬

본 논문의 주요 목적은 말초동맥 질환 빈번 발생 동맥에서 말초 동맥 질환을 식별하기 위한 혈압 파형 기반 딥러닝 진단 모델을 개발하는 것이다. 데이터 기반 방식으로 일반화된 말초동맥 질환 진단 모델을 얻기 위해서는 2가지 문제점이 있다: 1) 질환 심각도와 발병 위치의 차이로 인한 도메인 불일치, 2) 말초동맥 질환 초기 증상이 없다는 특징으로 인한 데이터 불균형. 실제 문제를 고려하여 일반화된 말초동맥 질환 진단 모델 훈련을 위해, 최대 분류 불일치 방법에 두가지 보조 테스크를 추가한 지도 도메인 적응 방법을 제안한다. 제안된 모델은 다양한 질병 심각도 수준에서 전송 선로 모델에서 생성된 가상 환자의 혈압파형을 사용하여 검증된다. 결과는 제안된 모델이 다양한 질병 심각도 수준에서 PAD 위치를 식별하기 위한 우수한 성능을 가지고 있음을 보여준다. 이 결과는 다양한 질병 심각도에서 하지의 PAD 위치를 식별하기 위해 제안된 진단 모델을 실제 병원에 적용할 가능성을 나타낸다.

주제어: 심혈관 질환(Cardiovascular Disease)
말초동맥 질환(Peripheral Arterial Disease)
파형 분석(Pulse Waveform Analysis)
딥 러닝(Deel Learning)
도메인 적응(Domain Adaptation)

학 번: 2020-25983